

Lévy noise induced transitions and enhanced stability in a birhythmic van der Pol system

René Yamapi^{1,2,a}, Raoul Mbakob Yonkeu³, Giovanni Filatrella⁴, and Jürgen Kurths^{2,5}

¹ Fundamental Physics Laboratory, Physics of Complex System Group, Department of Physics, Faculty of Science, University of Douala, P.O. Box 24157, Douala, Cameroon

² Potsdam Institute for Climate Impact Research (PIK), 14473 Potsdam, Germany

³ Laboratory of Mechanics and Materials, Department of Physics, Faculty of Science, University of Yaoundé I, P.O. Box 812, Yaoundé, Cameroon

⁴ Department of Sciences and Technologies and Salerno unit of CNSIM, University of Sannio, Via Port'Arsa 11, 82100 Benevento, Italy

⁵ Department of Physics, Humboldt University, 12489 Berlin, Germany

Received 22 January 2019 / Received in final form 29 April 2019

Published online 10 July 2019

© EDP Sciences / Società Italiana di Fisica / Springer-Verlag GmbH Germany, part of Springer Nature, 2019

Abstract. This work describes the effects of Lévy noise on a birhythmic van der Pol like oscillator. The two periodic attractors are characterized by different periods, and the stability in the presence of Gaussian noise can be described by an effective, or quasi-potential. Numerical simulations demonstrate that in the presence of Lévy noise the induced escapes from an attractor to another are similar to the escapes between stable points in an ordinary potential. Assuming that the attractors are almost separated by a barrier of a quasi (or pseudo) potential, the theory for Lévy noise escapes captures the qualitative features of the escapes across the quasi-potential. The differences to the Gaussian case are more pronounced for large values of the Lévy index. We found that for the symmetric quasi-potential, the relative stability of the two attractors are similar, while in the asymmetric case the properties of the two attractors differ for increasing α . The global stability is also characterized by means of the residence times, that give indications for future theoretical analysis.

1 Introduction

Lévy noise is a preeminent example of non-Gaussian noise. The underlying notion is that some noise sources, or random signals, are not characterized by a finite variance. Moreover, if one makes the further requirement that the noise distribution is stable, i.e., it is the limit distribution of the sum of many random and identically distributed variables, the resulting distribution belongs to the family of Lévy functions, as a generalization of the central limit theorem [1]. The presence of anomalous, non-thermal (Gaussian) noise is widely recognized in physical systems and practical devices. In the natural world, Lévy noise has been modeled for most different systems, such as in predator-pray systems [2]. Quite naturally, Lévy noise often appears in telecommunications and networks [3] where noise (from diverse sources as atmospheric disturbances, relay contacts, electromagnetic devices, electronic apparatus, transportation systems, switching transients, and accidental hits in telephone lines [4]) can exhibit impulsive and Lévy-type characteristics. In mechanical

systems, Lévy fluctuations have been also used to describe vibration data in industrial bearings [5–7]. Another example of the relevance of anomalous distributions in material issues has been proposed in photoluminescence experiments of moderately doped n-InP samples [8], and the presence of Lévy flights could prove to have an impact on the design of some optoelectronic devices [9]. On the fundamental side Lévy processes can reveal properties in the electron transport [10] and optical properties [11–13] of semiconducting nanocrystals quantum dots. Transport properties can be connected with Lévy superdiffusion [14], e.g. in the quasiballistic heat conduction [15,16]. Lévy noise produces some further peculiar effects [17–20]. For example, it has been shown that the nonlinear relaxation dynamics of three different systems of condensed matter exhibit stochastic resonant activation and the noise-induced coherence of electron spin [17,18]. In biological models of a stepping molecular motor, subject to the influence of symmetric, white Lévy noise that mimics the action of external random forcing [19], it appears that as noise parameters are changed, speed and direction appear to depend very sensitively upon the characteristics of the noise. In population dynamics it has been shown

^a e-mail: ryamapi@yahoo.fr

that the transient dynamics of the Verhulst model perturbed by arbitrary non-Gaussian white noise depends upon the initial delta function distribution [20]. It has been found a transition induced by multiplicative Lévy noise, from a trimodal probability distribution to an asymptotic bimodal probability distribution, and also to a nonmonotonic behavior of the nonlinear relaxation time as a function of the Cauchy stable noise intensity.

A special role is played by Lévy noise in oscillators. Most important for the electrical power grid is the noise from wind turbines rotation parts [21], that can severely affect the infrastructure stability. Also in superconducting active oscillators as superconducting Josephson junctions [22], Lévy noise has been advocated, e.g., in graphene based devices in the form of rare jumps of the voltage response of such a non-linear oscillator [23] or when the electron–electron interaction of the graphene under the effects of a laser source gives rise to a random walk with a Lévy flight distribution [24]. In nonlinear oscillators the effect of Lévy noise, and indeed of Gaussian noise as well, is subtle, in the sense that the stable solution is a dynamical attractor. When this is the case, and the force cannot be derived as the gradient of a potential function, the problem of stability cannot be deduced from the standard escape from a potential well, as characterized by an *Arrhenius* behavior of the lifetime as a function of the noise intensity. However, an alternative approach based on the concept of an effective potential (a pseudo, or quasi-potential) has proved to be effective to treat the consequences of noise on the metastable periodic attractor for nonlinear oscillators as Josephson junctions [25–27] and for van der Pol birhythmic oscillators [28–30], also in the presence of correlated noise [31]. It is therefore quite natural to extend the theory of Lévy noise-induced escapes from ordinary potentials [32,33] to quasi-potentials for birhythmic van der Pol-like systems. In doing so, one follows the approach for monorhythmic systems already employed using the principle of minimum action [34,35], that describes a numerical method to derive the quasi-potential for a non-gradient system. The conceptual difficulty to follow this line of reasoning is that the distance rather than the energy barrier matters. Moreover, this line of research is numerically heavy. An analytic approach has been presented for an ordinary, non-birhythmic van der Pol system (with Lévy noise) [36–38], and also extended to a birhythmic system [39].

In this work, we use numerical methods already employed for Gaussian noise, that is to revert the logic of the escape time in the presence of Lévy noise [40,41]. In doing so we intend to determine whether the quasi-potential concept is applicable to birhythmic systems, and to ascertain the limits of the applicability of this concept. Also, one wishes to ascertain if numerical simulations can carry information about the theoretical estimates of the features of escapes from ordinary potentials, in particular the dependence of the escape times on the Lévy index, α .

The paper is organized as follows. Section 2 describes the birhythmic van der Pol system driven by Lévy noise and the algorithm of numerical simulations. After the description of the main features of the deterministic birhythmic van der Pol oscillator and the parameter

region where birhythmicity appears, the Lévy’s process and numerical algorithm conclude this section. Section 3 contains the algorithm to generate random Lévy noise and integrate the corresponding stochastic differential equation, also the numerical results on the rates, that are the basis to retrieve the global stability properties of the attractors. For the low noise regime, the Arrhenius factor (i.e., the relation between the escape time $\langle T_{esc} \rangle$ and the noise intensity D) allows to determine an effective activation energy barrier ΔU from the slope of the linear part of the variation in the escape time versus the inverse noise intensity. Section 4 is devoted to conclusions.

2 The stochastic birhythmic system in the presence of Lévy noise

In this section, the model underlying the birhythmic oscillations is described. Also, the analytic considerations that lead to the quasi-potential in the Gaussian case are given, and the numerical method to solve the stochastic equations in the presence of Lévy noise is presented.

2.1 The birhythmic van der Pol system

The model considered is a van der Pol-like oscillator with a nonlinear function of higher polynomial order described by the following nonlinear equation (overdots as usual stand for the derivative with respect to time)

$$\ddot{x} - \mu(1 - x^2 + \alpha x^4 - \beta x^6) \dot{x} + x = 0, \quad (1)$$

where the quantities α and β are positive parameters that indicate the system behavior, for instance in the biochemical interpretation of model (1) [42,43] to a ferroelectric instability compared with its electrical resistance, and μ is a positive parameter that tunes nonlinearity [42–45]. Equation (1) describes several dynamic systems, ranging from physics to engineering and biochemistry [45–47]. In particular equation (1) seems to be more appropriate for some biological processes than the classical van der Pol oscillator, as shown in [48]. When employed to model biochemical systems, namely the enzymatic-substrate reactions, x in equation (1) is proportional to the population of enzyme molecules in the excited polar state. Model (1) is therefore a prototype for self-sustained systems and exhibits interesting features of nonlinear dynamical systems. In references [42,43] the super-harmonic resonance structure was analyzed and symmetry-breaking crisis and intermittency was found. The nonlinear dynamics and the synchronization process of two such systems was investigated in references [44,45], the possibility that introducing an active control of chaos can be tamed for an appropriate choice of the coupling parameters was considered in reference [46], while the effects of external an excitation on the multi-limit cycle van der Pol system was analyzed in reference [31]. It appears that the birhythmic behavior is still present for a very small excitation and disappears when the amplitude of the driven becomes large.

The nonlinear self-sustained oscillator equation (1) possesses more than one stable limit-cycle solution [48], a

condition for the occurrence of birhythmicity. Birhythmic systems are of interest, for example in biology, to describe the coexistence of two stable oscillatory states, a situation that can be found various enzyme reactions [49] or in circadian models [50–52]. Another example is the explanation of the existence of multiple frequency and intensity windows in the reaction of biological systems to irradiation with very weak electromagnetic fields [43,48,53–56]. This work focuses on model (1) as a prototype for the occurrence of birhythmicity, rather than on the special features of a single realization.

2.2 Analytic considerations

Following references [44,45], the periodic solutions of equation (1) can be approximated, if the nonlinearity is mild ($\mu \ll 1$) by

$$x(t) = A \cos \omega t. \quad (2)$$

The analytic amplitude A and frequency ω can be readily obtained [44,45]. It has been found that the amplitude A is independent of the parameter μ , which only enters in the frequency ω . The amplitude equation is given by

$$\frac{5\beta}{64}A^6 - \frac{\alpha}{8}A^4 + \frac{1}{4}A^2 - 1 = 0, \quad (3)$$

and the frequency ω by:

$$\omega = 1 + \mu^2\omega_2 + o(\mu^3), \quad (4)$$

with

$$\begin{aligned} \omega_2 = & \frac{93\beta^2}{65536}A^{12} - \frac{69\alpha\beta}{16384}A^{10} + \left(\frac{67\beta}{8192} + \frac{3\alpha^2}{1024}\right)A^8 \\ & - \left(\frac{73\beta}{2048} + \frac{\alpha}{96}\right)A^6 + \left(\frac{1}{128} + \frac{\alpha}{24}\right)A^4 - \frac{3}{64}A^2. \end{aligned}$$

Depending on the value of α and β , the van der Pol birhythmic system (1) possesses one or three limit cycles. When three limit cycles are obtained, two of them are stable and one is unstable, a condition for birhythmicity; the unstable limit cycle represents the separatrix between the basins of attraction of the two stable limit cycles. This is shown in Figure 1, with the bifurcation lines that contour the region of existence of birhythmicity in the two parameter phase space ($\alpha - \beta$) [44,45]. The bifurcation line on the left denotes the passage from a single limit cycle to three limit cycles, while the right one denotes the reverse passage from three limit cycles to a single solution. At the conjunction, a codimension-two bifurcation, or cusp, appears. The first bifurcation encountered increasing the parameter α corresponds to a saddle-node bifurcation of the outer or larger limit cycle amplitude, while the second bifurcation occurs in correspondence of a saddle-node bifurcation of the inner or smaller amplitude cycle. The two frequencies associated with the limit cycles are very close to the lowest amplitude A bifurcation and clearly distinct at the highest a bifurcation line. In Figure 1 the

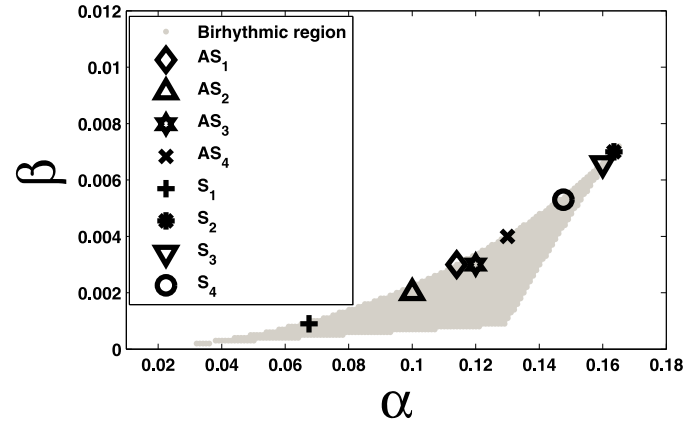


Fig. 1. Parameter region of the single limit cycle (white area) and three limit cycles (gray area) with $\mu = 0.01$ as obtained from simulations of equation (3). The symbols refer to the parameter sets investigated in this work, see Tables 1 and 2. The other parameter is $\mu = 0.01$.

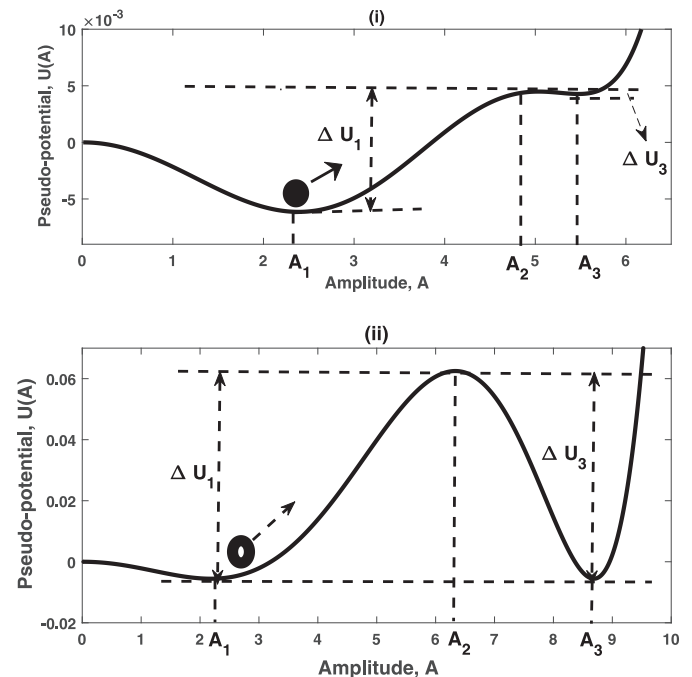


Fig. 2. The effective pseudo-potential $U(A)$ versus the amplitude A for the free-noise self-sustained oscillator with multi-limit-cycles; (i) corresponds to the asymmetric potential with the AS_1 parameters, while (ii) to the symmetric potential with the S_1 parameters. The other parameter is $\mu = 0.01$.

range of existence of birhythmic solutions in the parameter plane (α, β) is shown; Examples of the corresponding pseudo-potential are shown in Figure 2: (i) the first type is an asymmetric pseudo-potential with different potential wells (such as in Fig. 2i); (ii) and the second type is a symmetrical potential (see Fig. 2ii) and here the depths of the two potential wells are almost identical. In Tables 1 and 2, the amplitudes of the limit cycles in both cases are reported, for some selected values of α and β . The two sets of parameters: AS_1 for the asymmetric quasi-potential and

$$\Phi(k) = \begin{cases} \exp \left\{ i\delta k - \sigma^a |k|^a (1 - ib \operatorname{sgn}(k) \tan(\frac{a\pi}{2})) \right\} & \text{for } a \neq 1, 2, \\ \exp \left\{ i\delta k - \sigma |k| (1 + ib \frac{2}{\pi} \operatorname{sgn}(k) \ln |k|) \right\} & \text{for } a = 1, \\ \exp \left\{ i\delta k - \frac{1}{2} \sigma^2 k^2 \right\} & \text{for } a = 2, \end{cases} \quad (5)$$

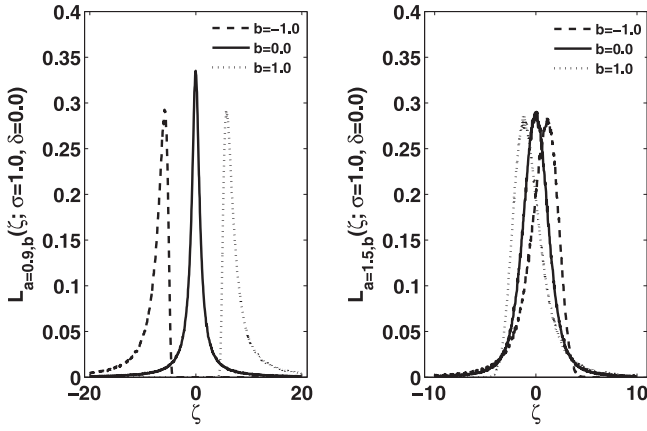


Fig. 3. Sample a-stable probability density functions with $a = 0.9$ (left panel) and $a = 1.5$ (right panel). For $b = 0$ the distributions are symmetric, while for $b \neq 0$ they are asymmetric functions.

S_1 for the symmetric quasi-potential are further explored in this work.

2.3 The Lévy process representation

Lévy distributions, that describe the noise we consider in this work, are a rich class of probability distributions with several intriguing mathematical properties [57]. The Lévy process can be viewed as a generalized Wiener process that follows the Lévy distribution $L_{a,b}(\zeta, \sigma, \delta)$; its representation is given by the characteristic function defined in the Fourier transform $\Phi(k)$ [58]:

See equation (5) above

where a ($0 < a \leq 2$) denotes the stability Lévy index; for $a = 2$ the Lévy stable distribution is the standard Gaussian distribution. The parameter b ($b \in [-1; +1]$) is an asymmetry, or skewness parameter, namely, the Lévy distribution is symmetric for $b = 0.0$ and asymmetric for $b \neq 0.0$, δ ($\delta \in \mathbb{R}$) is the center or location parameter which denotes the mean value of the distribution, and which exists and reads as $1 < a \leq 2$ [58]. The parameters σ ($\sigma \in]0; +\infty[$) and $D = \sigma^a$ are the scale parameter and noise intensity, respectively [59,60]. The van der Pol oscillator is used to describe ferroelectric oscillations, D has the physical meaning of the intensity of the random electric field.

The random variables ξ corresponding to the characteristic functions (5) can be generated by the following algorithm [61,62]: first one generates a random variables U uniformly distributed in $[-\frac{\pi}{2}, +\frac{\pi}{2}]$ and a variable W exponentially distributed with a unit mean; U and W

Table 1. Amplitudes of the limit cycles and quasi-potential barriers $\Delta U_{1,3}$ for the asymmetric potential. All data refer to the case $\mu = 0.01$ and $D = 0.0$. All the results are obtained analytically.

$AS_i = (a, \beta)$	Amplitudes	Quasi-potential barriers ΔU_i
$AS_1 = (0.114, 0.003)$	$A_1 = 2.37720$	$\Delta U_1 = 1.062 \times 10^{-2}$
	$A_2 = 5.02638$	$\Delta U_3 = 2.111 \times 10^{-4}$
	$A_3 = 5.46665$	
$AS_2 = (0.1, 0.002)$	$A_1 = 2.3069$	$\Delta U_1 = 1.437 \times 10^{-2}$
	$A_2 = 4.8472$	$\Delta U_3 = 4.423 \times 10^{-2}$
	$A_3 = 7.1541$	
$AS_3 = (0.12, 0.003)$	$A_1 = 2.4269$	$\Delta U_1 = 4.989 \times 10^{-2}$
	$A_2 = 4.2556$	$\Delta U_3 = 2.372 \times 10^{-2}$
	$A_3 = 6.3245$	
$AS_4 = (0.13, 0.004)$	$A_1 = 2.4903$	$\Delta U_1 = 4.342 \times 10^{-3}$
	$A_2 = 4.4721$	$\Delta U_3 = 4.237 \times 10^{-4}$
	$A_3 = 5.0791$	

Table 2. Amplitudes of the limit cycles and quasi-potential barriers $\Delta U_{1,3}$ for the symmetric potential. All data refer to the case $\mu = 0.01$ and $D = 0.0$. All the results are obtained analytically.

$S_i = (a, \beta)$	Amplitudes	Quasi-potential barriers ΔU_i
$S_1 = (0.0675, 0.0009)$	$A_1 = 2.1730001$	$\Delta U_1 = 6.5085 \times 10^{-2}$
	$A_2 = 6.3245003$	$\Delta U_3 = 6.5085 \times 10^{-2}$
	$A_3 = 8.6760004$	
$S_2 = (0.1635, 0.007)$	$A_1 = 3.0925001$	$\Delta U_1 = 2.376 \times 10^{-5}$
	$A_2 = 3.5280002$	$\Delta U_3 = 2.445 \times 10^{-5}$
	$A_3 = 3.9190002$	
$S_3 = (0.16, 0.00658)$	$A_1 = 2.9520001$	$\Delta U_1 = 1.0345 \times 10^{-4}$
	$A_2 = 3.5965002$	$\Delta U_3 = 1.1011 \times 10^{-4}$
	$A_3 = 4.1535002$	
$S_4 = (0.1476, 0.0053)$	$A_1 = 2.6905001$	$\Delta U_1 = 8.6713 \times 10^{-4}$
	$A_2 = 3.8525002$	$\Delta U_3 = 8.7677 \times 10^{-4}$
	$A_3 = 4.7405002$	

being statistically independent. The Lévy distributed variable X can be generated as follows:

For $a \neq 1$:

$$X = S_{a,b} \frac{\sin(a(U + B_{a,b}))}{(\cos(U))^{1/a}} \left(\frac{\cos(U - a(U + B_{a,b}))}{W} \right)^{\frac{1-a}{a}}, \quad (6)$$

where

$$\begin{cases} B_{a,b} = \frac{\arctan(b \tan(a\pi/2))}{a}, \\ S_{a,b} = (1 + (b \tan(a\pi/2))^2)^{\frac{1}{2a}}. \end{cases} \quad (7)$$

For $a = 1$:

$$X = \frac{2}{\pi} \left[\left(\frac{\pi}{2} + bU \right) \tan U - b \log \left(\frac{a\pi W \cos U}{2bU + a\pi} \right) \right]. \quad (8)$$

Finally, the abovementioned ξ reads:

$$\xi = \begin{cases} \sigma X + \delta, & a \neq 1, \\ \sigma X + 2b\sigma \frac{\log(\sigma)}{2} + \delta, & a = 1. \end{cases} \quad (9)$$

The Lévy noise is a formal time derivative of the generalized Wiener process. For the time step of integration Δt , the increments of the generalized Wiener process are distributed according to the distribution $L(\xi, \sigma \Delta t^{1/a}, \delta)$. The Lévy process can be retrieved with the transformation $\zeta(t) = \Delta t^{1/a} \xi$ [61,62]. Lévy probability densities functions under different stability indexes and skewness parameters are presented in Figure 3: they are symmetric for $b = 0$; for $a < 1$, $L(\xi, \sigma \Delta t^{1/a}, \delta)$ instead they are left-skewed for $b < 0$ and right-skewed for $b > 0$. For $a > 1$, $L(\xi, \sigma \Delta t^{1/a}, \delta)$ is right-skewed for $b < 0$ and left-skewed for $b > 0$.

2.4 The numerical method to simulate the birhythmic van der Pol system driven by Levy noise

It is here assumed that the model system is subject to a random excitation governed by the Langevin version of equation (1):

$$\ddot{x} - \mu(1 - x^2 + \alpha x^4 - \beta x^6)\dot{x} + x = \zeta(t), \quad (10)$$

where $\zeta(t)$ denotes the Lévy noise and it is the formal time derivative of a Lévy process $\xi(t)$, obeying to the Lévy distribution $L(\xi, \sigma \Delta t^{1/a}, \delta)$, where the Lévy noise measures for instance the intensity of the random electrical field. Introducing a new variable $\dot{x} = u$, equation (10) can be written in the form:

$$\begin{cases} \dot{x} = u, \\ \dot{u} = \mu(1 - x^2 + \alpha x^4 - \beta x^6)u - x + \zeta(t), \end{cases} \quad (11)$$

and the following relative difference scheme [57] is obtained to simulate the system (11):

$$\begin{cases} x_{n+1} - x_n = u_n \Delta t, \\ u_{n+1} - u_n = [\mu(1 - x_n^2 + \alpha x_n^4 - \beta x_n^6)u_n - x_n] \Delta t + \Delta t^{1/a} \xi, \end{cases}$$

where ξ denotes Lévy distributed random number with the stability Lévy index a and the noise intensity $D = \sigma^a$, as per equation (9). Simulations are performed with the time step $\Delta t = 0.01$ and for the sake of simplicity, for symmetric Lévy distributions, $\delta = b = 0$. In this analysis the number of realizations has been set to 100; a five-fold increase in the number of realizations in selected cases has demonstrated that the change of the logarithm of escape time is modest, of the order of 5%. We conclude that a substantial improvement calls for a drastic change in the speed of the simulations, possibly with CUDA techniques [63].

3 Global stability analysis

A principal question about the effects of noise is the occurrence of large deviations, i.e. excursions from one attractor to another. In fact, as an attractor is only locally stable, birhythmicity is displayed if the system moves from an attractor to the other. One is therefore interested in the global analysis, i.e. the time spent on average in the proximity of each attractor, that is in the average time to escape from an attractor towards the other. The natural approach for potential systems, when the force can be derived from the gradient of a function, is the classical Kramers theory, with various modifications which have been since developed. For non-gradient systems, the quasi-potential plays a similar role, inasmuch it determines the asymptotic low noise behavior of the escape times for Gaussian noise [64]. The quasi-potential has proved effective for the van der Pol birhythmic system driven by uncorrelated and correlated Gaussian noise, also in the presence of a sinusoidal forcing term [28,30,65,66]. Our goal is to study whether the same approach can be effective for Lévy noise.

3.1 Statement of the problem

A quasi-potential function $U(A)$ is an effective energy in the sense that it determines, in the low noise regime, the average escape time $\langle T_{esc}(D) \rangle$ from the attractor with an Arrhenius-like behavior [29]:

$$\langle T_{esc}(D) \rangle \propto \exp(\Delta U/D). \quad (12)$$

A number of questions arise in the extension of equation (12) to birhythmic van der Pol under Lévy noise influence. First, one can ask how to modify the functional form of equation (12). The escapes are governed, for Lévy noise systems with a bona fide potential [40,41,67,68], by the expression

$$\langle T_{esc}(a, D) \rangle \simeq \left(\frac{\eta^{1-\mu_a} \Delta z^{2-2\mu_a+a\mu_a}}{4^{1-\mu_a} \Delta U^{1-\mu_a} 2^{a\mu_a}} \right) \frac{\mathcal{C}_a}{D^{\mu_a}}, \quad (13)$$

where Δz is the distance between the stable minimum of the potential and the separatrix, ΔU is the energy or the activation barrier, η the damping index (that only appears to correctly normalize the overdamped equation), a the index of the Lévy distribution, and D the noise intensity. The scaling exponent μ_a and the coefficient \mathcal{C}_a are supposed to have a universal behavior for overdamped systems [40]. The coefficient \mathcal{C}_a theoretical behavior reads [40] 1 for $a \rightarrow 0$, passes through $\pi/2$ for $a = 1$, and diverges as $1/(2-a)$ as the Lévy parameter approaches $a = 2$. The coefficient μ_a can be approximated as follows [40]:

$$\mu_a \simeq 1 + 0.401(a-1) + 0.105(a-1)^2. \quad (14)$$

The adaptation of equation (13) to the van der Pol birhythmic system gives a first analytical result on the influence of Lévy noise. In other words, in equation (13) z can be interpreted as a generic coordinate where the force

stems from a potential. As such, z cannot be the variable x of equation (5), that is a non-potential (or non-gradient) ordinary differential equation, and hence U does not exist. To apply the theory of Lévy noise [32,33] to equation (5) it is necessary to introduce an effective potential that plays the role of U through a change of the dynamics variable. How to calculate the same potential for Lévy noise is still an open problem. We hypothesize that the effective potential can be approximated by the quasi-potential derived with the stochastic averaging method for Gaussian noise:

$$\frac{dA}{dt} = -\frac{dU(A)}{dA} + \sqrt{\tilde{D}}\zeta_1(t), \quad (15)$$

where the amplitude A of the oscillations as per equation (2) is an effective coordinate, $\zeta_1(t)$ is the Gaussian noise, \tilde{D} an effective noise amplitude $\tilde{D} = D/\omega^2$ [30]. In this approximation the effective potential $U(A)$ is given by [30]:

$$U(A) = \frac{\mu}{128} \left(\frac{5\beta}{8} A^8 - \frac{4\alpha}{3} A^6 + 4A^4 - 32A^2 \right) - \frac{\tilde{D}}{2} \ln(A). \quad (16)$$

Moreover, we further assume that $\tilde{D} \simeq 0$ in equation (16). In this approximation, Δz , the distance with the separatrix in equation (13), becomes $A_2 - A_1$ and $A_3 - A_2$ for the outer and inner barriers, respectively, the damping reads $\eta = 1$, and one can tentatively apply the theory [40] to equation (15), with $\zeta_1(t)$ a Lévy noise. This is a very rough approximation, but gives an analytical prediction to be compared with numerical data.

Numerical simulations have been performed to verify the accuracy of the above approximations. To do so, one could revert the logic of equation (13) to determine the energy activation. This approach leads to the following definition of quasi-potential:

$$\Delta U \equiv \frac{\eta}{4} \left(\frac{\Delta x^{2-2\mu_a+a\mu_a}}{\langle T_{esc}(a, D) \rangle 2^{a\mu_a}} \right)^{\frac{1}{1-\mu_a}} \left(\frac{C_a}{D^{\mu_a}} \right)^{\frac{1}{1-\mu_a}}. \quad (17)$$

This procedure is rather cumbersome, for Lévy escapes are almost independent of the potential height, that only appears in the prefactor of equation (13). It is anyway interesting to verify if, and to which extent, the behavior of equation (13) is reproduced by the numerically retrieved confining energy. The prefactor is the most delicate point in the calculations [36–38]. To underline the effects, one can rewrite equation (13) as follows:

$$\begin{aligned} \log[\langle T_{esc}(a, D) \rangle] &= \log \left[\frac{\eta^{1-\mu_a}}{4^{1-\mu_a} 2^{a\mu_a}} \right] + \log \left[\frac{\Delta A^{2-2\mu_a+a\mu_a}}{\Delta U^{1-\mu_a}} \right] \\ &\quad + \log[C_a] - \mu_a \log[D]. \end{aligned} \quad (18)$$

When the barrier is changed the main contribution arises from ΔA , as $\mu_a \simeq 1$.

The agreement is poor; however, the very fact that the escapes follow the functional form of a power law (rather

than an exponential), as shown in the numerical calculations is *per se* of interest, because it demonstrates that the Lévy noise induces a qualitative change in the outcome of the system.

3.2 Escape times from the periodic attractors

The Lévy noise term in equation (9) induces the system to occasionally jump from one limit cycle to the other. The purpose of this Section is to determine the escape times from the periodic attractors under the effect of such noise term. The system, being initially on a limit-cycle attractor with amplitude A_1 or A_3 , is thus forced by random fluctuations to leave the attractor and to wander about in the neighboring state space. An escape occurs when this random motion drives the system across the boundary of the basin of attraction or the unstable limit cycle with amplitude A_2 , (i.e. $|x| > A_2$ (respectively, $|x| < A_2$)) over the activation energy ΔU_1 (respectively, ΔU_3). This energy is provided by the random force, that thus furnishes the energy equivalent to the depth of the left (respectively, right) well of the bistable potential. The mean escape times $\langle T_{esc} \rangle$ for the transitions $A_1 \rightarrow A_3$ and $A_3 \rightarrow A_1$ as a function of the noise intensity D for the asymmetric and symmetric pseudo-potentials are shown in Figures 6 and 7, for several different values of the Lévy index a ($0.1 \leq a \leq 2$). We generally observe that for both types of potential, the curves for $\alpha < 2$ obey a different law in comparison to the Gaussian counterpart. Earlier studies have shown that the variation of the escape time depends on the regime of the noise intensity to be considered. For a low noise intensity regime, in addition to the exponential dependence of the inverse of the intensity of the noise, $1/D$, as it appears in Figures 4–7 demonstrate a power-law asymptotic behavior, as predicted by equation (13). These figures refer to both the symmetric and asymmetric cases of the pseudo-potentials. A thorough analysis of the data of the results presented in Figures 6 and 7 allows us to show the dependencies of the coefficient C_a and the power-law exponent μ_a on the Lévy index a in Figures 8 and 9, respectively. In Figure 8 the theoretical estimate for the coefficient C_a reads 1 for $a \rightarrow 0$, passes through $\pi/2$ for $a = 1$, and diverges as $1/(2-a)$ as the Lévy parameter approaches 2 [33]. The agreement is but qualitative, as can be seen from the data of Figure 8, that does not start from 0 as expected for $a \rightarrow 0$, reads 1 instead of $\pi/2$ for $a = 1$, and diverges more mildly than expected. In numerical investigation, C_a reads 0.15 for the index parameter approaching 0.01. In Figure 9, the dependence of the scaling exponent μ_a versus the Lévy index a is compared to the analytical approximation (14). For both the symmetric and asymmetric pseudo-potential, the estimate is acceptable. One can conclude that the prefactor C_a is only qualitatively captured by the estimate for the ordinary potential, while the scaling exponent μ_a seems to be closer to the ordinary potential predictions.

The influence of the noise intensity on the escape process is shown in Figures 10 and 11 in dependence on the mean escape time T_{esc} versus the Lévy index a , for several different values of the noise intensity, D , for the asymmetric and symmetric pseudo-potential.

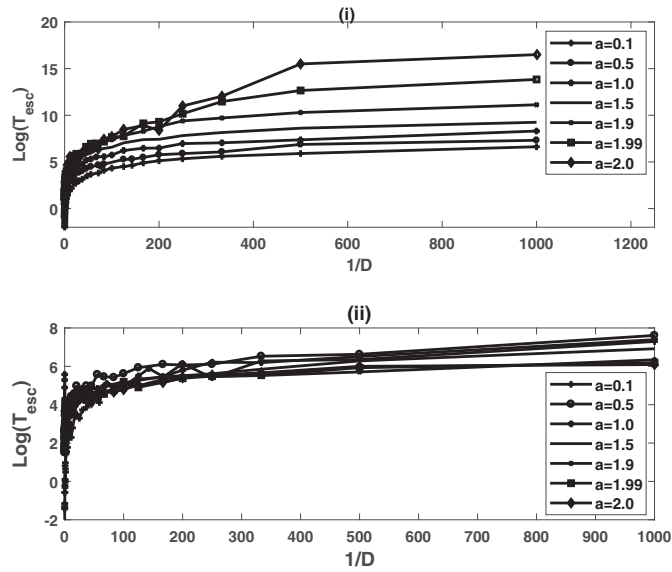


Fig. 4. Mean escape time versus the noise intensity $1/D$ for the asymmetric quasi-potential with several different values of the Lévy index, a ; (i) corresponds to the escape transition $A_1 \rightarrow A_3$ and (ii) to the escape transition $A_3 \rightarrow A_1$. The other parameters are $\mu = 0.01$; $\alpha = 0.114$; $\beta = 0.003$.

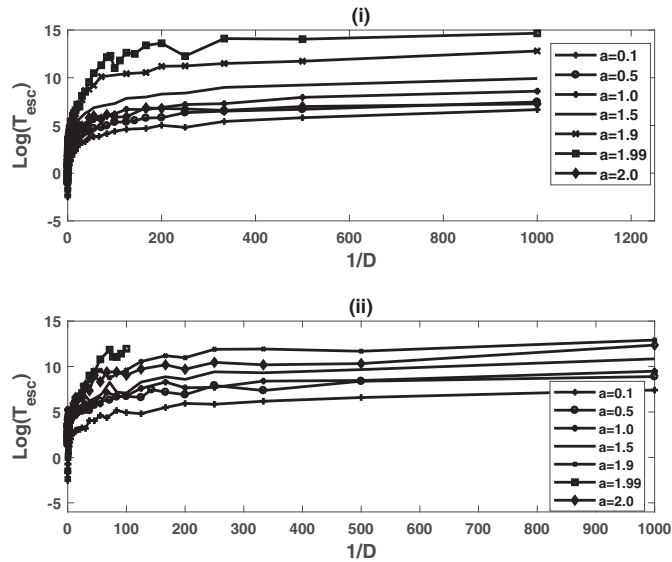


Fig. 5. Mean escape time versus the noise intensity $1/D$ for the symmetric quasi-potential with several different values of the Lévy index, a ; (i) corresponds to the escape transition $A_1 \rightarrow A_3$ and (ii) to the escape transition $A_3 \rightarrow A_1$. The other parameters are $\mu = 0.01$; $\alpha = 0.0675$; $\beta = 0.0009$.

As it is often expected, increasing the noise intensity reduces the escape time in both types of potential. However, the observations strongly depend on the Lévy index a ; it appears that for a very small value of D , for example $D = 0.001$, the escape time increases or decreases considerably when the Lévy index is close to 2, that is close to the Gaussian case. For example, in the case of the asymmetric pseudo-potential, the escape transition time $\langle T_{esc} \rangle(A_1 \rightarrow A_3)$ (or $\langle T_{esc} \rangle(A_3 \rightarrow A_1)$) when

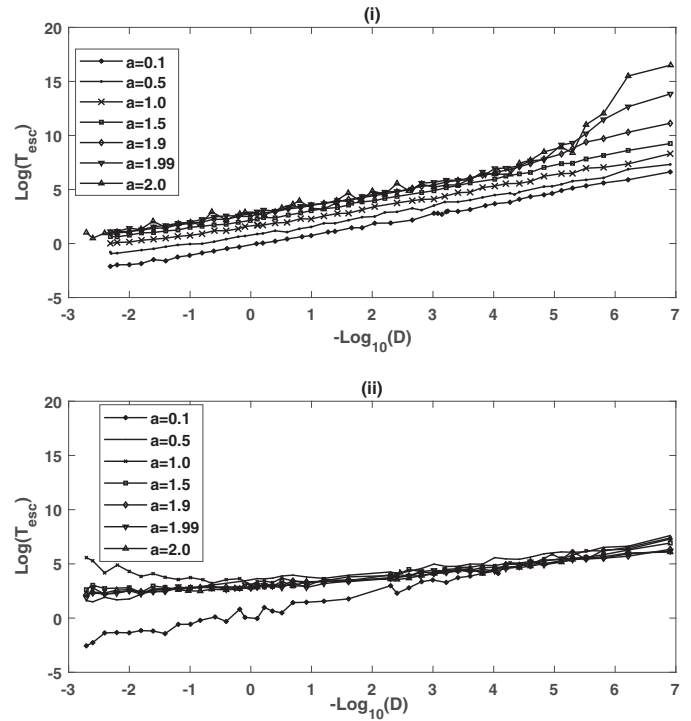


Fig. 6. Mean escape time versus the noise intensity D for the asymmetric quasi-potential with several different values of the Lévy index, a ; (i) corresponds to the escape transition $A_1 \rightarrow A_3$ and (ii) to the escape transition $A_3 \rightarrow A_1$. The other parameters are $\mu = 0.01$; $\alpha = 0.114$; $\beta = 0.003$.

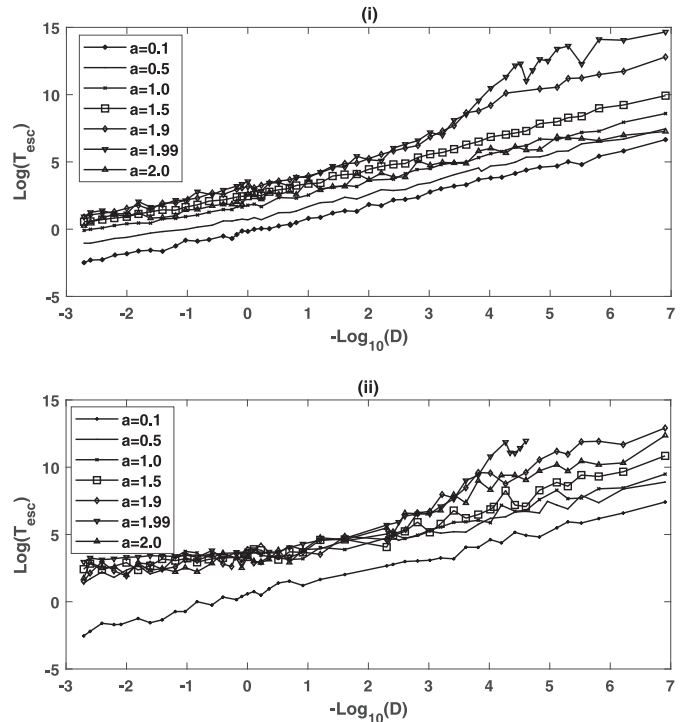


Fig. 7. Mean escape time versus the noise intensity D for the symmetric quasi-potential with several different values of the Lévy index, a ; (i) corresponds to the escape transition $A_1 \rightarrow A_3$ and (ii) to the escape transition $A_3 \rightarrow A_1$. The other parameters are $\mu = 0.01$; $\alpha = 0.0675$; $\beta = 0.0009$.

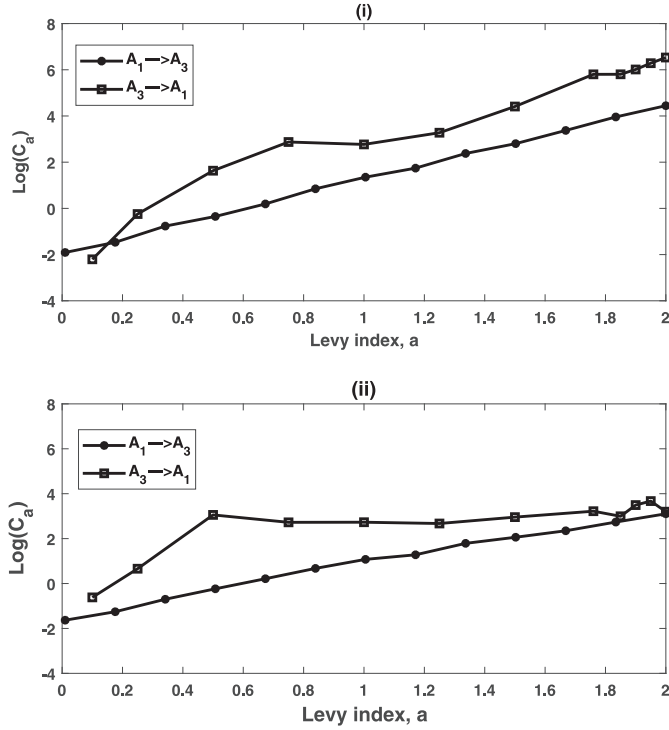


Fig. 8. Dependence of the scaling exponent C_a versus the Lévy index, a ; (i) corresponds to the asymmetric pseudo-potential (with $\alpha = 0.114$; $\beta = 0.003$) and (ii) for the symmetric pseudo-potential (with $\alpha = 0.0675$; $\beta = 0.0009$). The other parameter is $\mu = 0.01$.

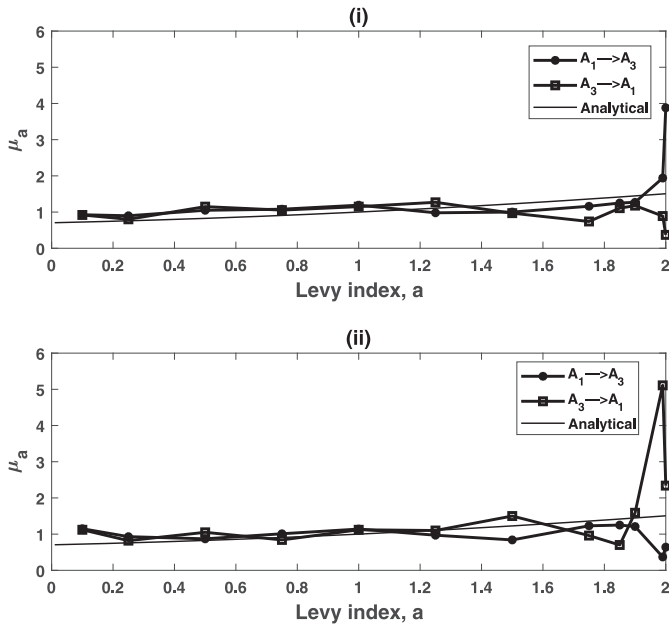


Fig. 9. Dependence of the scaling exponent μ_a versus the Lévy index, a ; (i) corresponds to the asymmetric pseudo-potential (with $\alpha = 0.114$; $\beta = 0.003$) and (ii) to the symmetric pseudo-potential (with $\alpha = 0.0675$; $\beta = 0.0009$). The analytic prediction of the solid line refers to equation (14). The other parameter is $\mu = 0.01$.

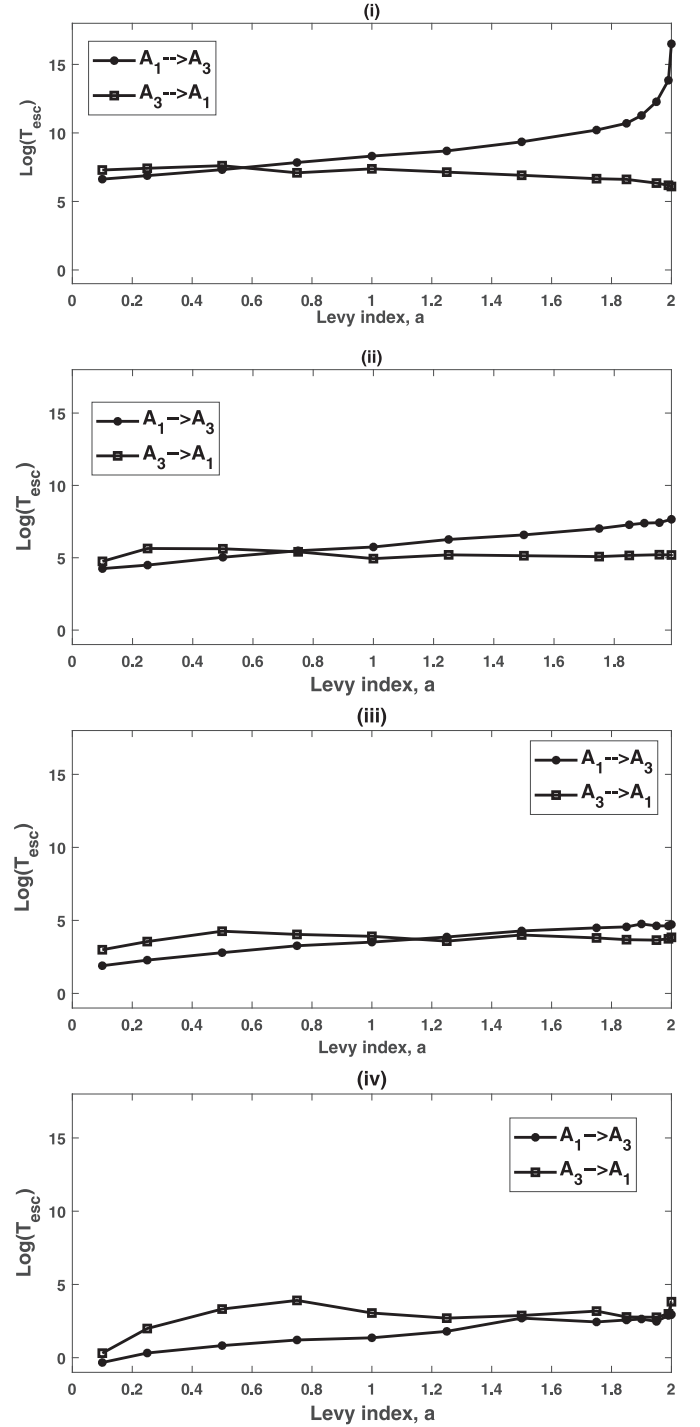


Fig. 10. Effects of the Lévy noise intensity on the variation of the mean escape time versus the Lévy index a for the asymmetric quasi-potential; (i) $D = 0.001$; (ii) $D = 0.01$; (iii) $D = 0.1$; (iv) $D = 1.0$. The other parameters are $\mu = 0.01$; $\alpha = 0.114$; $\beta = 0.003$.

the Lévy index changes from 0.1 to 2, the escape time passes from 7.6×10^2 to 1.4×10^8 (from 1.4×10^3 to 4.9×10^2 , respectively). This is reported in Table 3, that displays the dependence of the escape times as a function

Table 3. Escape times for the asymmetric pseudo-potential with low noise intensity $D = 0.001$. All data refer to the case $\mu = 0.01$ and the following van der Pol parameters: $\alpha = 0.114$; $\beta = 0.003$.

Levy index a	$T_{esc}(A_1 \rightarrow A_3)$	Estimate equation (13)	$T_{esc}(A_3 \rightarrow A_1)$	Estimate equation (13)
0.1	7.5×10^2	1.3×10^2	1.5×10^3	3.6×10^2
0.25	9.7×10^2		1.7×10^3	
0.5	1.5×10^3		2.0×10^3	
0.75	2.5×10^3		1.2×10^3	
1.0	4.1×10^3	3.0×10^2	1.6×10^3	1.8×10^3
1.25	5.9×10^3		1.3×10^3	
1.5	1.1×10^4		1.0×10^3	
1.75	2.5×10^4		7.8×10^2	
1.9	7.3×10^5		5.9×10^2	
1.99	1.0×10^7	1.1×10^7	4.8×10^2	3.9×10^8

Table 4. Escape times for the symmetric pseudo-potential with low noise intensity $D = 0.001$. All data refer to the case $\mu = 0.01$ and the following van der Pol parameters: $\alpha = 0.0675$; $\beta = 0.0009$.

Levy index a	$T_{esc}(A_1 \rightarrow A_3)$	Estimate equation (13)	$T_{esc}(A_3 \rightarrow A_1)$	Estimate equation (13)
0.1	7.7×10^2	1.7×10^2	1.6×10^3	2.3×10^2
0.25	1.0×10^3		2.3×10^3	
0.5	1.7×10^3		7.3×10^3	
0.75	3.0×10^3		1.0×10^4	
1.0	5.4×10^3	7.2×10^2	1.3×10^4	3.3×10^2
1.25	9.1×10^3		1.4×10^4	
1.5	2.0×10^4		4.9×10^4	
1.75	6.4×10^4		4.3×10^4	
1.9	3.6×10^4		4.0×10^5	
1.99	2.3×10^7	1.8×10^5	2.9×10^7	5.6×10^5

of the Lévy index. In the case of a symmetric pseudo-potential, one observes the same behavior when the Lévy index increases, see Table 4 for a much more in-depth look at the dependence of escape time versus the Lévy index, a . It should be noted that in this case the pseudo-potential is symmetric without the Lévy noise term, (i.e. $T_{esc}(A_1 \rightarrow A_3) \simeq T_{esc}(A_3 \rightarrow A_1)$) and becomes asymmetric in the presence of this noise and returns symmetric as $a \rightarrow 2$ that corresponds to the Gaussian case. It can be seen that when the Lévy index a increases from 0.1 to 2.0, the escape time to leave the pseudo-potential well around the limit cycle amplitude A_3 increases very considerably and makes the attractor A_3 more stable under the effect of the Lévy noise. As a result, a particle confined in this pseudo-potential remains for a very long time under the effects of the random fluctuations induced by the Lévy noise.

Numerical simulations can be used to show the effect of the Levy index a on the pseudo-potential associated with equation (13), that is on the global stability properties of the attractors. In other words, one can estimate from numerical simulations the average time that a particle confined in the potential well spends to move to the other well. The analytic approximations developed in the previous section can thus be checked against numerical results. A discrepancy is to be expected, for the theory of the Lévy noise has not been fully extended to the pseudo-potentials. Figure 12 presents the comparison between the numerical studies and the analytical results, for the transitions in the two cases of symmetric and asymmetric pseudo-potentials.

We find that the comparison between the analytical and numerical results is acceptable for the Lévy $a = 0.1$, but the agreement progressively deteriorates when the index a increases.

3.3 Residence times as a measure of global stability properties

The local stability of the attractors with different frequencies that characterize birhythmicity is not sufficient to determine the global properties of the system under the influence of noise that drives the system from an orbit to the other. To characterize the whole system and the overall behavior, including the transitions from an attractor to the other, it is useful to compute the average persistence or residence time $R_{1,3}$ on the attractor with limit-cycle amplitude $A_{1,3}$ as

$$R_j = \frac{T_j}{T_1 + T_3}, \quad j = 1, 3 \quad (19)$$

where $T_{1,3}$ is the average escape time from the first attractor A_1 , i.e. $T_1 = T_{esc}(A_1 \rightarrow A_3)$, or from the third attractor A_3 , i.e. $T_3 = T_{esc}(A_3 \rightarrow A_1)$. Figures 13 and 14 show the effects of the noise intensity on the residence times $R_{1,3}$ as a function of a for the asymmetric and the symmetric pseudo-potentials, respectively. For the case of an asymmetric pseudo-potential (i.e. the parameters AS_1), for noise intensity around $D = 1/1000$ and with the Lévy index $a = 0.1$, one gets $R_3(a = 0.1) = 0.6598$,

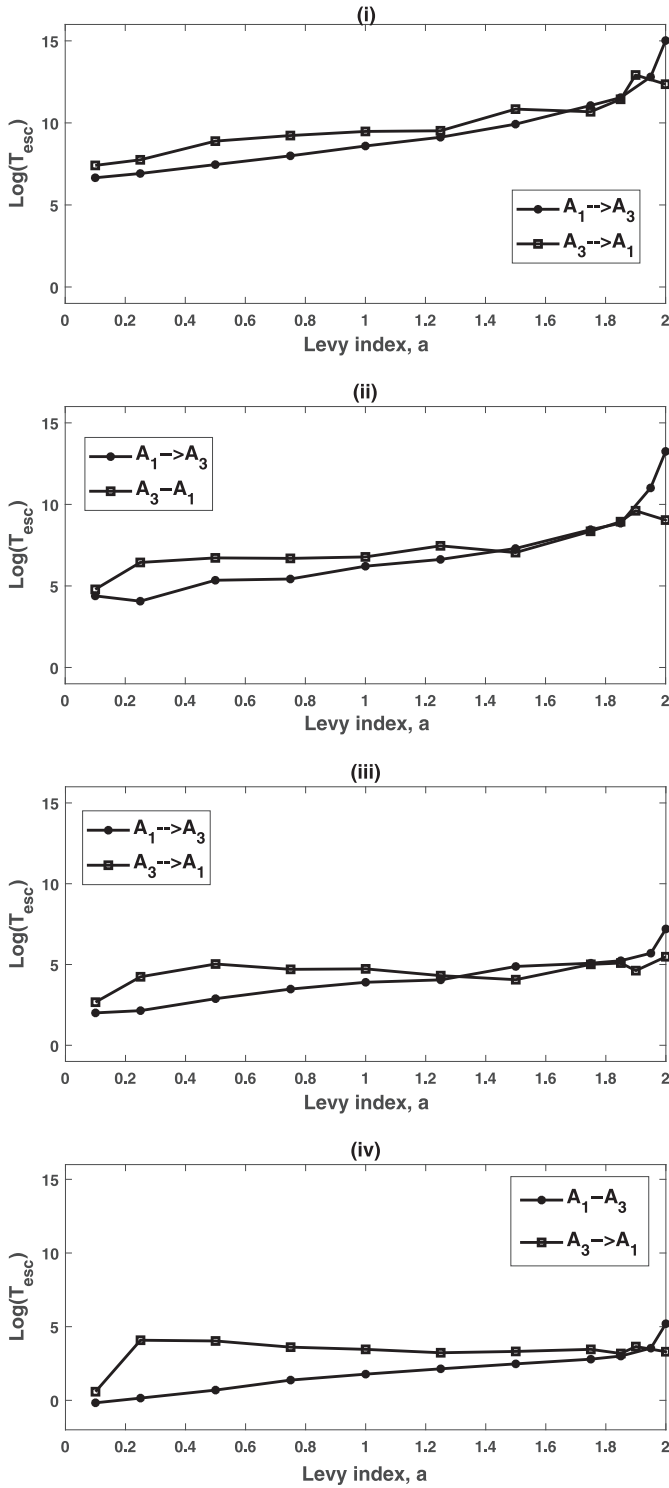


Fig. 11. Effects of the Lévy noise intensity on the variation of the mean escape time versus the Lévy index a for the symmetric quasi-potential; (i) $D = 0.001$; (ii) $D = 0.01$; (iii) $D = 0.1$; (iv) $D = 1.0$. The other parameters are $\mu = 0.01$; $\alpha = 0.0675$; $\beta = 0.0009$.

and conversely $R_1(a = 0.1) = 0.3402$ (see Fig. 13). Put it in other words, the system spends about 66% of the time on the third attractor A_3 and 34% on the first

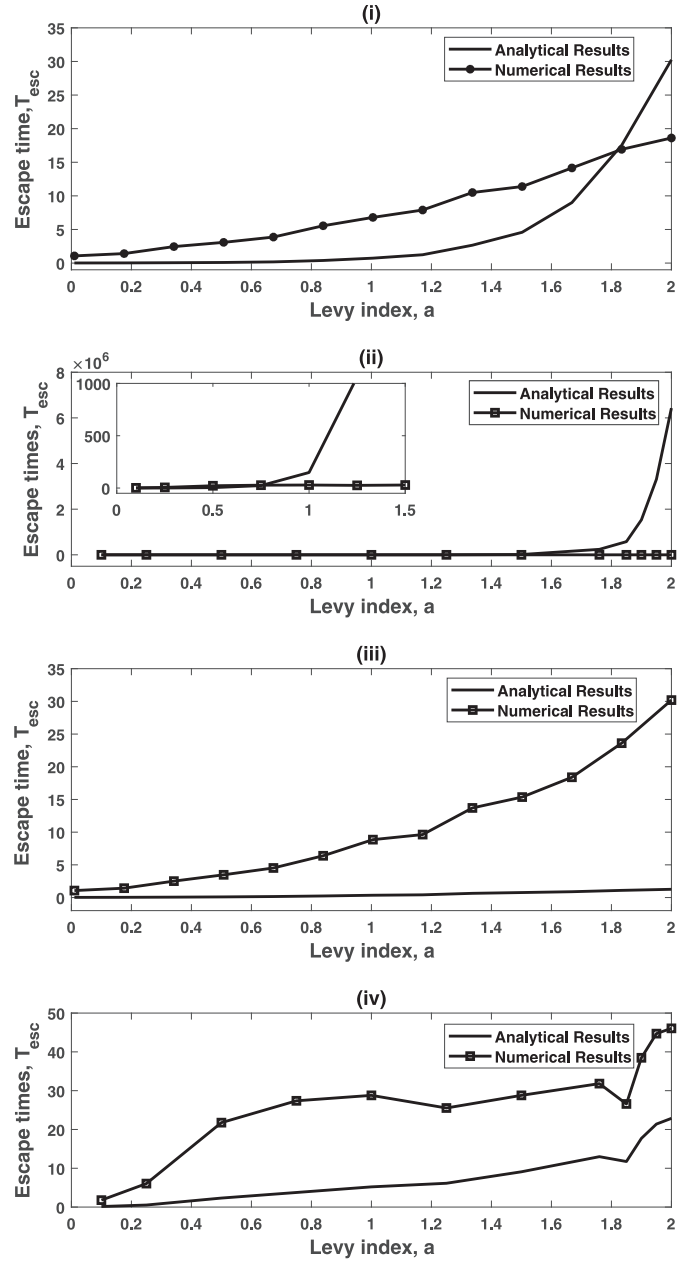


Fig. 12. Comparison between analytical and numerical results for (i); (ii) asymmetric quasi-potential (with $\alpha = 0.114$; $\beta = 0.003$), (iii), (iv) symmetric potential (with $\alpha = 0.0675$; $\beta = 0.0009$). (i,ii) $A_1 \rightarrow A_3$; (ii,iv) $A_3 \rightarrow A_1$ with $D = 1.0$.

attractor A_1 . Increasing a , the residence time on attractor A_1 increases, while that on attractor A_3 decreases. It appears in Figure 13i that at $a = 0.6$ the system spends about the same time on both attractors A_1 and A_3 , i.e. $R_1(a = 0.6) \simeq R_3(a = 0.6)$. A further increase of the Lévy index causes R_1 to increase while R_3 decreases. A change of the intensity of the noise, i.e. $D = 1/100$, leaves the scenario unchanged, but for the value of the index $a = 0.7$ at which the system spends the same time on both attractors, (i.e., $R_1 \simeq R_3$). Figure 14 shows the variation of the residence times $R_{1,3}$ as a function of a for the symmetric pseudo-potential, with two values of the noise intensity:

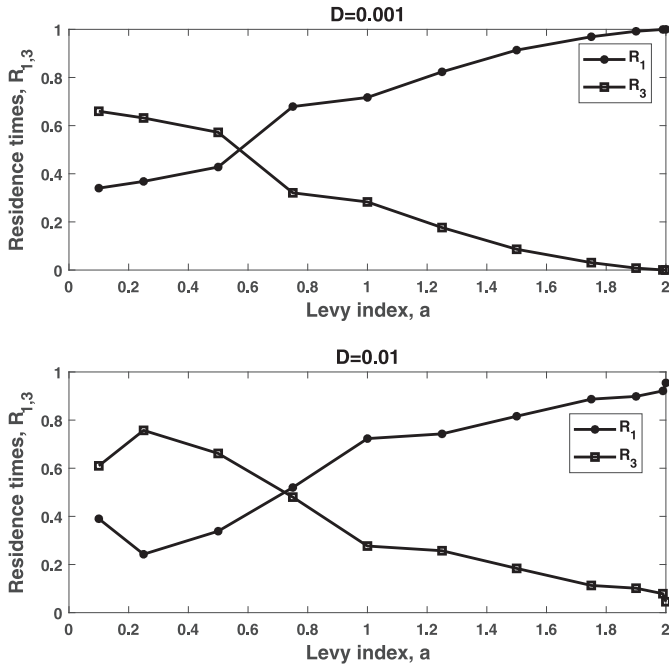


Fig. 13. Residence times $R_{1,3}$ as a function of the Lévy index, a for different values of the noise intensity, D , for the asymmetric quasi-potential. The other parameters are $\mu = 0.01$; $\alpha = 0.114$; $\beta = 0.003$.

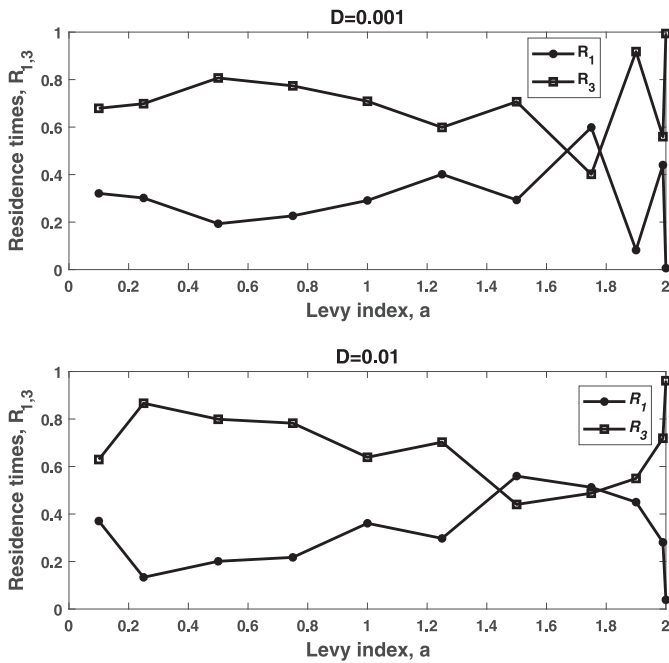


Fig. 14. Residence times $R_{1,3}$ as a function of the Lévy index, a for different values of the noise intensity, D , for the symmetric quasi-potential. The other parameters are $\mu = 0.01$; $\alpha = 0.0675$; $\beta = 0.0009$.

$D = 1/1000$ and $D = 1/100$. Unlike the case of asymmetric pseudo-potential, the system spends more time on the attractor A_3 , for $R_3 > R_1$ at almost all values of the parameter a . Only close to the Lévy index $a \simeq 2$ the role of

the two attractors exchange, and the attractor A_1 becomes dominant for $R_1 > R_3$.

4 Conclusions

The effects of Lévy noise on a prototypical birhythmic van der Pol system have been studied through numerical simulations. The self-sustained oscillator is a convenient model that displays birhythmic properties and it is particularly tractable with stochastic averaging for the Gaussian noise case. This work focuses on the occurrence of large deviations, that is on excursions from an attractor to another under the perturbation of Lévy noise. The Lévy noise escapes from an ordinary potential are governed by the law equation (13), that depends also on the noise intensity D and the Lévy index parameter a . The mean escape time $\langle T_{esc} \rangle$ to escape from one limit-cycle attractor to the other has been proposed as a measure of the attractor's global stability. The agreement with the predictions based on the quasi-potential analytically derived in the case of Gaussian noise is poor. Even the qualitative agreement is generally confirmed, with the noticeable exception of the transitions from the outer attractor to the inner one for the asymmetric quasi-potential. However, a systematic collection of the numerical escape times gives some indications for the dynamics. Most importantly, the escape times appear to be very different for the two attractors and to be significantly depending on the Lévy index, a .

As the quasi-potential derived for the Gaussian case seems to be not accurate in describing the Lévy noise induced escapes, a more direct measure of the relative stability for the two attractors has been employed: the numerical evaluation of the residence times (19). With this tool one can highlight the role of the Lévy noise parameter a ; it is found that for the symmetric quasi-potential, the index changes leave the relative stability of the two attractors almost unchanged (see Fig. 14), while in the asymmetric case the properties of the two attractors are exchanged increasing a (see Fig. 13).

Let us conclude with an outlook on other possible approaches to the determination of the quasi-potential. One is to use the principle of minimum action [34,35]. These authors describe a numerical method to derive the quasi-potential for a non-gradient system. The physical idea, that has also been used for Josephson junctions [26,27], is that noise activated trajectories have a different weight, and that the minimum energy is the most likely to be followed by the noise driven system. However, this line of research is numerically heavy, and might also prove not appropriated for Lévy noise, where the distance rather than the energy barrier matters. Another promising avenue is perhaps to follow the line of thinking of the calculations for the ordinary van der Pol system (with Lévy noise) [36–38] that, interestingly, has also been applied to another birhythmic system with two attractors [39] to derive a quasi-potential rather than an ordinary potential.

It would be interesting to search for the existence of noise enhanced stability (NES) phenomenon [69] in the case of Lévy noise system characterized by a quasi-potential, as the one associated to birhythmic van der Pol.

So far, in the preliminary simulations performed, it has not been found a clear signature of stability enhanced by noise. One can conclude that, at variance with the ordinary potential, systems characterized by a quasi-potential do not exhibit NES. However, the exploration has just begun and we cannot exclude that such a phenomenon exists.

R.Y. undertook this work with the support of the German Academic Exchange Service(DAAD), Germany. He acknowledges the support of the Potsdam Institute for Climate Impact Research (PIK), Potsdam, Germany. The authors thank Claudio Guarcello for enriching contributions.

Author contribution statement

R. Yamapi conceived the main idea and prepared the manuscript. All authors contributed to the analysis of the numerical results, read and approved the final manuscript.

References

1. A.A. Dubkov, B. Spagnolo, V. Uchaikin, *Int. J. Bifurcat. Chaos* **18**, 2649 (2008)
2. A. La Cognata, D. Valenti, A.A. Dubkov, B. Spagnolo, *Phys. Rev. E* **82**, 011121 (2010)
3. X. Yang, A.P. Petropulu, *IEEE Trans. Signal Process.* **51**, 64 (2003)
4. V. Bhatia, B. Mulgrew, A. Georgiadis, *Signal Process.* **86**, 835 (2006)
5. C. Li, G. Yu, in *2010 Second International Conference on Computer Modeling and Simulation* (2010), Vol. 4, p. 386
6. R. Saadane, M.E. Aroussi, M. Wahbi, in *3rd International Renewable and Sustainable Energy Conference (IRSEC)* (2015), p. 1
7. B. Chouri, M. Fabrice, A. Dandache, M.E. Aroussi, R. Saadane, in *International Conference on Multimedia Computing and Systems (ICMCS)* (2014), p. 1545
8. S. Luryi, O. Semyonov, A. Subashiev, Z. Chen, *Phys. Rev. B* **86**, 201201 (2012)
9. A.V. Subashiev, O. Semyonov, Z. Chen, S. Luryi, *Phys. Lett. A* **378**, 266 (2014)
10. D.S. Novikov, M. Drndic, L.S. Levitov, M.A. Kastner, M.V. Jarosz, M.G. Bawendi, *Phys. Rev. B* **72**, 075309 (2005)
11. X. Brokmann, J.-P. Hermier, G. Messin, P. Desbiolles, J.-P. Bouchaud, M. Dahan, *Phys. Rev. Lett.* **90**, 120601 (2003)
12. M. Kuno, D.P. Fromm, H.F. Hamann, A. Gallagher, D.J. Nesbitt, *J. Chem. Phys.* **115**, 1028 (2001)
13. G. Messin, J.P. Hermier, E. Giacobino, P. Desbiolles, M. Dahan, *Opt. Lett.* **26**, 1891 (2001)
14. R. Metzler, J. Klafter, *Phys. Rep.* **339**, 1 (2000)
15. A.M.S. Mohammed, Y.R. Koh, B. Vermeersch, H. Lu, P.G. Burke, A.C. Gossard, A. Shakouri, *Nano Lett.* **15**, 4269 (2015)
16. B. Vermeersch, A.M.S. Mohammed, G. Pernot, Y.R. Koh, A. Shakouri, *Phys. Rev. B* **91**, 085203 (2015)
17. G. Augello, D. Valenti, B. Spagnolo, *Eur. Phys. J. B* **78**, 225 (2010)
18. B. Spagnolo, D. Valenti, C. Guarcello, A. Carollo, B. Di Paola, *Chaos, Solitons Fractals* **81**, 412 (2015)
19. B. Lisowski, D. Valenti, B. Spagnolo, M. Bier, E. Gudowska-Nowak, *Phys. Rev. E* **91**, 042713 (2015)
20. A.A. Dubkov, B. Spagnolo, *Eur. Phys. J. B* **65**, 361 (2008)
21. Y. Elyassami, K. Benjelloun, M. El Aroussi, *Contemp. Eng. Sci.* **9**, 453 (2016)
22. A. Barone, G. Paternó, *Physics and Applications of the Josephson Effect* (Wiley, New York, 1982)
23. C. Guarcello, D. Valenti, A. Carollo, B. Spagnolo, *J. Stat. Mech.: Theory Exp.* **2016**, 054012 (2016)
24. U. Briskot, I.A. Dmitriev, A.D. Mirlin, *Phys. Rev. B* **89**, 075414 (2014)
25. R. Yamapi, G. Filatrella, *Phys. Rev. E* **89**, 052905 (2014)
26. R.L. Kautz, *Phys. Rev. A* **38**, 2066 (1988)
27. R.L. Kautz, *J. Appl. Phys.* **76**, 5538 (1994)
28. R. Yamapi, G. Filatrella, M.A. Aziz-Alaoui, H.A. Cerdeira, *Chaos* **22**, 043114 (2012)
29. R. Yamapi, G. Filatrella, M.A. Aziz-Aloui, *Chaos* **20**, 013114 (2010)
30. R. Mbakob Yonkeu, R. Yamapi, G. Filatrella, C. Tchawoua, *Commun. Nonlinear Sci. Numer. Simul.* **33**, 70 (2016)
31. R. Mbakob Yonkeu, R. Yamapi, G. Filatrella, C. Tchawoua, *Physica A* **466**, 569 (2017)
32. A.V. Chechkin, V.Y. Gonchar, M. Szydlowsky, *Phys. Plasmas* **9**, 78 (2002)
33. A.V. Chechkin, V.Yu. Gonchar, *Zh. Eksp. Teor. Fiz.* **118**, 3 (2000)
34. Y. Sun, X. Zhou, [arXiv:1701.04044v6](https://arxiv.org/abs/1701.04044v6)
35. X. Wan, B. Zheng, G. Lin, *Commun. Comput. Phys.* **23**, 408 (2018)
36. M. Högele, I. Pavlyukevich, *Stochastic Anal. Appl.* **32**, 163 (2014)
37. M. Högele, I. Pavlyukevich, [arXiv:1405.5433v1](https://arxiv.org/abs/1405.5433v1)
38. M. Högele, I. Pavlyukevich, *Stochastics Dyn.* **15**, 1550019 (2015)
39. F. Morán, A. Goldbeter, *Biophys. Chem.* **20**, 149 (1984)
40. A.V. Chechkin, V.Yu. Gonchar, J. Klafter, R. Metzler, *Europhys. Lett.* **72**, 354 (2005)
41. A.V. Chechkin, O.Yu. Sliusarenko, R. Metzler, J. Klafter, *Phys. Rev. E* **75**, 041101 (2007)
42. F. Kaiser, C. Eichwald, *Int. J. Bifurcat. Chaos* **1**, 485 (1991)
43. C. Eichwald, F. Kaiser, *Int. J. Bifurcat. Chaos* **1**, 711 (1991)
44. H.G. Enjieu Kadji, R. Yamapi, J.B. Chabi Orou, *Chaos* **17**, 033113 (2007)
45. H.G. Enjieu Kadji, J.B. Chabi Orou, R. Yamapi, P. Wofo, *Chaos, Solitons Fractals* **32**, 862 (2007)
46. R. Yamapi, B.R. Nana Nbandjo, H.G. Enjieu Kadji, *Int. J. Bifurcat. Chaos* **17**, 1343 (2007)
47. H.G. Enjieu Kadji, *Synchronization dynamics of nonlinear self-sustained oscillations with applications in physics, engineering and biology*, PhD Dissertation of Physics, Institut de Mathématiques et de Sciences Physiques (I.M.S.P.), Porto-Novo, Université d'Abomey-Calavi, Benin, June 2006
48. F. Kaiser, *Radio Sci.* **17**, 17S (1981)
49. V.-X. Li, A. Goldbeter, *J. Theor. Biol.* **138**, 149 (1989)
50. M.E. Jewett, D.B. Forger, R.E. Kronauer, *J. Biol. Rhythms* **14**, 493 (1999)

51. P. Indic, D.B. Forger, M.A. St. Hilaire, D.A. Dean II, E.N. Brown, R.E. Kronauer, E.B. Klerman, M.E. Jewett, *Chronobiol. Int.* **22**, 613 (2005)
52. S. Hartzell, M.S. Bartlett, L. Virgin, A. Porporato, J. Theor. Biol. **368**, 83 (2015)
53. F. Kaiser, *Coherent Excitations in Biological Systems: Specific Effects in Externally Driven Self-Sustained Oscillating Biophysical Systems* (Springer-Verlag, Berlin, Heidelberg, 1983)
54. F. Kaiser, in *Biological Effects and Dosimetry of Nonionizing Radiation*, edited by M. Grandolfo, S.M. Michaelson and A. Rindi (Plenum Press, NY, 1983), p. 251
55. F. Kaiser, in *Energy Transfer Dynamics*, edited by T.W. Barret, H.A. Pohl (Springer, Berlin, 1987), p. 224
56. F. Kaiser, *Kleinheubacher Berichte* **32**, 395 (1989)
57. D. Applebaum, *Lévy Processes and Stochastic Calculus*, 2nd edn. (Cambridge University Press, New York, 2009)
58. R. Weron, *Int. J. Mod. Phys. C* **12**, 209 (2001)
59. A. Janicki, A. Weron, *Simulation and chaotic behavior of α -stable stochastic processes* (Marcel Dekker, New York, 1994)
60. A. Janicki, *Numerical and Statistical Approximation of Stochastic Differential Equations with Non-Gaussian Measures* (HSC Monograph, Wroclaw, 1996)
61. Y. Xu, Y. Li, J. Li, J. Feng, H. Zha, *J. Stat. Phys.* **158**, 131, (2015)
62. K. Jacobs, *Stochastic processes for physicists: Understanding Noisy Systems* (Cambridge University Press, New York, 2010)
63. V. Pierro, L. Troiano, E. Mejuto, G. Filatrella, *J. Comput. Phys.* **361**, 136 (2018)
64. R. Graham, T. Tél, *Phys. Rev. A* **31**, 1109 (1985)
65. R. Yamapi, A. Chéagé Chamgoué, G. Filatrella, P. Wofo, *Eur. Phys. J. B* **90**, 153 (2017)
66. R. Mbakob Yonkeu, R. Yamapi, G. Filatrella, C. Tchawoua, *Nonlinear Dyn.* **84**, 627 (2016)
67. C. Guarcello, D. Valenti, B. Spagnolo, V. Pierro, G. Filatrella, *Nanotechnology* **28**, 134001 (2017)
68. C. Guarcello, D. Valenti, B. Spagnolo, V. Pierro, G. Filatrella, *Phys. Rev. Appl.* **11**, 044078 (2019)
69. N.V. Agudov, A.A. Dubkov, B. Spagnolo, *Physica A* **325**, 144 (2003)